© JUL 2026 | IRE Journals | Volume 10 Issue 1 | ISSN: 2456-8880
DOI: https://doi.org/10.64388/IREV10I1-1720170

Stabilization of Low Earth Orbit Satellite Attitude Control System Using Robust Proportional-Integral-Derivative-Tuned Compensator

MUOGHALU, C. N.[1], ACHEBE, P. N.[2], PATRICK, U. P.[3], IDAM, E. O.[4]
[1,2]*Department of Electrical/Electronic Engineering, Chukwuemeka Odumegwu Ojukwu University, Uli, Anambra State, Nigeria*
[3]*Department of Electrical/Electronic Engineering, Federal Polytechnic, Oko, Anambra State, Nigeria*
[4]*Department of Electrical/Electronics Engineering, Joseph Sarwuan Tarka University, Makurdi, Benue State, Nigeria*

Abstract: The impact of effective satellite attitude control system (SACS) is that it can ensure both quality and reliability of data acquisition by a low earth orbit (LEO) satellite. This work presents design of adaptive controller for satellite y-axis attitude control system (ACS). With several techniques proposed in literature, there is still need to improve the tracking error and robustness of the control system in the presence of disturbance. In order to achieve this, the transfer function models of amplifier, actuator, and satellite structure for determining the transfer function a LEO satellite yaw-axis attitude were obtained. This work presents a yaw-axis ACS for LEO satellite using Proportional Integral and Derivative Tuned Compensator (PID-TC). The compensator was designed using the control system toolbox of MATLAB based on PID Tuning design method using robust response time tuning technique with interactive (adjustable performance and robustness) design mode at a bandwidth of 44.5 rad/s. The compensator was added to position control loop of yaw-axis. Simulations were carried out in MATLAB environment for four separate cases by applying unit forced input to examine the various step responses. Initial simulation without the inclusion of the compensator (PID-TC) in the control loop resulting in rise time of 2.16 s, settling time of 22.14 s and 38.63% overshoot. Thus, in terms of the performance criteria defined for the system, all conditions were not met specifically the settling time and the overshoot. Hence, a PID-TC controller was designed and introduced into the system, which resulted in transient and steady-state performances of the system being characterized by rise time of 3.82, settling time of 7.30 s, overshoot of 3.88%, and steady-state error (0). Generally, simulation results revealed that the proposed PID-TC controller meets all the performance criteria for a typical controller for LEO satellite yaw-axis attitude control system as defined in previous studies. The robustness of the designed PID-TC was examined by introducing a unit disturbance load torque and the step response simulation plot indicated that the achieved reduced rise time (1.82 s) and settling time (6.90 s) but with slight deterioration in smoothness and stability (as the overshoot was increased to 4.14%). When compared to the classical PID and Linear Quadratic Regulator (LQR), the PID-TC system provided the best dynamic response performance with in terms of convergence to steady-state (measured considering settling time), smoothness in response and stability both in the absence and presence of load torque disturbance. The significance of this work is that a robust PID-TC controller has been used to provide improved yaw angle (or attitude) tracking for LEO satellite in the absence and in the presence of load torque disturbance.

Keywords: Attitude Control System, Controller, LEO Satellite, PID Tuned Compensator, Yaw-Axis

I. INTRODUCTION

The orientation of satellite in space with respect to spacecraft communication is called attitude. Also, an on-orbit flight satellite control about its orientation axis is defined as attitude control. A satellite orbiting in space is called an on-orbit flight satellite. Thus, a set of devices forming a system including a subsystem such as the controller makes up attitude control system (ACS), which facilitates the determination and control on-orbit flight satellite. Enabling the accurate pointing of the satellite antenna at a given region of concern on earth and directing the solar panels towards the sun is the primary task in attitude control.

In accomplishing its tasks, the satellite's the control subsystem must be properly examined and then choose the method that ensures that the attitude adjustment and stability is achieve by improving transient or dynamic characteristics and steady-state performance (Eze and Ezenugu, 2024). This is because the performance of the satellite regarding meeting its expected tasks is directly determined by the effect of satellite attitude control (SAC) (Shan *et al*., 2022).

Since a satellite is subject to various disturbance on-orbit attitude and its reliability regarding data acquisition largely dependent on the effectiveness of the SAC system, several techniques are presented in previous studies for accurate satellite operation control. Usually, PID based techniques are implemented in several attitude or positioning such as in Onyekwelu *et al.* (2023), Okeya *et al.* (2024), Muoghalu *et al*. (2024), Muoghalu *et al*. (2021), and Muoghalu and Achebe (2021). Regarding yaw-axis attitude control, PID controller was used to meet performance specifications in yaw angle control of satellite system (Mbaocha *et al.,* 2016) and to stabilize the yaw-axis of microsatellite by minimizing Integral Time Absolute Error (ITAE) criteria (Ajiboye *et al.,* 2020). Similarly, other approaches involving the use of PID and its enhanced approaches in achieving attitude control regarding satellite yaw-axis are well documented as in Achebe and Muoghalu (2025), where additive mechanism was used. PID and fuzzy-PID controllers were separately used to carry out digital simulation of the SAC developed based on the mathematical model of satellite attitude, with PID offering faster steady-state though with evidence of certain torque oscillation while fuzzy-PID provided smother and improved stability in transient and steady-state performance response (Shan *et al.*, 2022). Muoghalu *et al* (2021) investigated enhancing DC motor speed stability by utilizing a chopper circuit, controlled by a PID algorithm, to manage voltage and counteract speed variations. Classical PD controller was replaced with FLC for yaw-axis closed loop reaction wheel of LEO microsatellite attitude stabilization (Benzeniar and Fellah, 2014). In the study carried out by Jin and Li (2022), integrated control method that is based on two-mode model predictive control (MPC) and using radiation pressure of sun from solar panels was used to achieve three-axis stabilization control of a spacecraft attitude that is under-actuated with two reaction wheels. Using variable structured PID controller, Qi et al. (2022) achieved attitude control satellites by integrating conventional PID model, trajectory planning, variable structure and fault tolerance. Okasha et al. (2019) used Lyapunov stability control theory to develop a control system for satellite attitude tracking system. Thruster and momentum wheels were employed by the ACS for satellite tracking.

In most of the previously yaw-axis ACS, the control system performance is largely subject or influenced by mismatch due to environmental disturbance or internal component parameter distortion because the effect of disturbance is not often modelled or factored in to the design. However, the developed control system attempts to factor in disturbance and thus has the ability to overcome the effect of unknown model uncertainties such as variation in system parameters due to gravitational and environmental impulses. The control technique developed in this work involves the use of PID tuning mechanism to optimize the performance of a compensator. Similar approach has been used by Onyeka *et al.* (2019), Eze *et al.* (2017), Muoghalu *et al*. (2020), and Muoghalu and Achebe (2025), respectively.

II. METHODS

2.1 Mathematical Modelling

In control system, mathematical modelling is used to describe the dynamic behaviour of a system being studied and this can be achieved by single or multiple equations depending on the components or complexity of the system. For the system shown in Figure 1, the components of the closed-loop control model for the yaw-axis ACS neglecting the PID-tuned compensator are: the amplifier, DC motor, and the satellite structure. Therefore, this subsection will focus on determining the mathematical model of the amplifier, DC motor and the satellite structure.

© JUL 2026 | IRE Journals | Volume 10 Issue 1 | ISSN: 2456-8880
DOI: https://doi.org/10.64388/IREV10I1-1720170

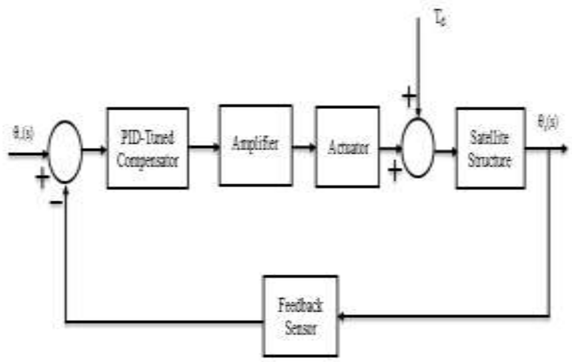

Figure 1: Closed loop of satellite yaw-axis ACS with torque disturbance

Mathematical Modelling of Amplifier

In control system and in many engineering applications, an amplifier is usually used to improve the strength or magnitude of the voltage to a usable value by the DC motor. In many applications, the amplifiers used have gain $k_a$and thus the output voltage is given by (Mbaocha et al., 2016):

$$V_a(s) = K_a V_i \quad (1a)$$

Hence, the open-loop gain of the amplifier can be expressed by:

$$K_a = \frac{V_a(s)}{V_i(s)} \quad (1b)$$

Mathematical Modelling of DC Motor

An armature controlled DC motor is schematically represented as shown in Figure 2. In the figure, DC motor is shown to have armature resistance and inductance $R_a$and L_a respectively, input or armature voltage,V_a, armature current I_a and motor back electromotive force (EMF) of $V_b$that make up the electrical component of the motor. The mechanical components are the motor moment of inertiaJ_a, damping ratio of the motor B_a, and the motor shaft angular position $\theta(t)$.

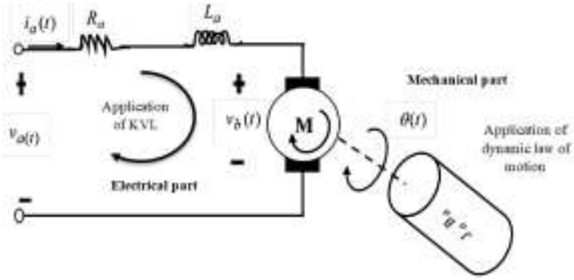

Figure 2: Schematic diagram of armature controlled DC motor (Eze *et al.,* 2021)

The application of Kirchhoff's voltage law (KVL) and the law of dynamic motion in the electrical and mechanical parts of the DC motor results in the following equations given by (Eze *et al.,* 2021; Akwukwaegbu *et al.,* 2023):

$$V_a(t) = R_a I_a(t) + L_a \frac{dI_a(t)}{dt} + V_b(t) \quad (2)$$

$$V_b(t) = K_b \omega_m(t) = K_b \frac{d\theta(t)}{dt} \quad (3)$$

$$T_m = K_m I_a \quad (4)$$

where ω_m is the motor angular speed and is equal to the derivation of the motor angular position or displacement, K_b is the motor back EMF constant, T_m is the motor toque, and $K_m$is the torque constant of the motor. Equation (4) can further be expressed by:

$$T_m = J_a \frac{d^2\theta(t)}{dt} + B_a \frac{d\theta(t)}{dt} \quad (5)$$

Now, substituting Equation (3) into Equation (2) and equating Equations (4) and (5), the following equations are established:

$$V_a(t) = R_a I_a(t) + L_a \frac{dI_a(t)}{dt} + K_b \frac{d\theta(t)}{dt} \quad (6)$$

$$J_a \frac{d^2\theta(t)}{dt} + B_a \frac{d\theta(t)}{dt} = K_m I_a \quad (7)$$

Taking the Laplace transform of Equations (6) and (7) and assuming zero initial conditions gives:

$$V_a(s) = L_a s I_a(s) + R_a I_a(s) + K_b s\theta(s) \quad (8)$$

$$J_a s^2\theta(s) + B_a s\theta(s) = K_m I_a(s) \quad (9)$$

Equating Equations (8) and (9) to eliminate the armature current gives:

$$\frac{V_a(s) - K_b s\theta(s)}{sL_a + R_a} = \frac{J_a s^2\theta(s) + B_a s\theta(s)}{K_m} \quad (10)$$

The constants K_b and K_m are usually given as $K_b = K_m = K$in most DC motor (Mbaocha et al., 2016). Therefore, Equation (10) can be expressed in terms of transfer function as the ratio of the motor angular position to the armature or input voltage given by:

$$\frac{\theta(s)}{V_a(s)} = \frac{K}{s[(J_a s + B_a)(L_a s + R_a) + K^2]} \quad (11)$$

Mathematical Model of Satellite System

The load torque T_L due to the torque delivered by the DC motor T_m and the disturbance torque T_d as shown Figure 3.2 is given by:

$$T_L = T_m + T_d \quad (12)$$

The moment of inertia J of the entire system consists of the motor moment of inertia $J_a$and the moment of inertia of the satellite structure or body J_l about axis of rotation at the centre of mass (Mbaocha et al., 2016). Given the associated vicious friction B of the satellite structure (i.e. the load) and its actual angular position

© JUL 2026 | IRE Journals | Volume 10 Issue 1 | ISSN: 2456-8880
DOI: https://doi.org/10.64388/IREV10I1-1720170

$\theta_o(t)$ about the yaw-axis, the load (satellite) torque assuming $T_d = 0$ is given by:

$$\boldsymbol{T_L = T_m = J\frac{d^2\theta_o(t)}{dt} + B\frac{d\theta_o(t)}{dt}} \quad (13)$$

The Laplace transform of Equation (13) assuming zero initial condition is given by:

$$\boldsymbol{T_m(s) = Js^2\theta_0(s) + Bs\theta_0(s)} \quad (14)$$

The transfer function of the satellite body dynamic in terms of the ration the actual angular position or attitude of the yaw-axis and input motor torque T_m (s) is given by:

$$\boldsymbol{\frac{\theta_o(s)}{T_m(s)} = \frac{1}{s(Js+B)}} \quad (15)$$

Substituting the values for the parameters in Table 1 into Equations (1b), (11) and (15) yields the numerical expressions for amplifier transfer function gain, the DC motor transfer function, and the satellite body transfer function as follows:

$$G_a(s) = \frac{V_a(s)}{V_i(s)} = 10 \quad (16)$$

$$G_m(s) = \frac{\theta(s)}{V_a(s)} = \frac{0.01}{0.05s^3+0.105s^2+0.0101s} = \frac{0.2}{s^3+2.1s^2+0.202s} \quad (17)$$

$$G_s(s) = \frac{\theta_o(s)}{T_m(s)} = \frac{1}{2.5s^2+1.17s} \quad (18)$$

The yaw-axis ACS is represented with a block diagram in terms of the transfer function of amplifier, DC motor, satellite body and unity gain feedback sensor assuming zero torque disturbance is shown in Figure 3 and the resulting transfer functions for open loop and closed control configuration of the yaw-axis ACS neglecting the PID-tuned compensator are given in Equations (19) and (20). Further modelling is considered assuming that unit torque disturbance enters the system as shown in Figure 4. The dynamic of the yaw-axis ACS with unit torque disturbance is divided into two parts as presented in Equation (21) without the compensator.

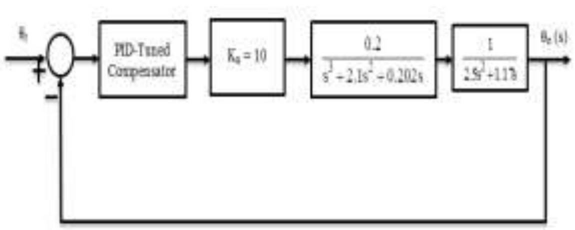

Figure 3: Closed loop network of satellite yaw-axis ACS with zero torque disturbance

$$G_{op}(s) = G_a(s) \times G_m(s) \times G_s(s) = \frac{2}{2.5\,s^5 + 6.42\,s^4 + 2.962\,s^3 + 0.2363\,s^2} \quad (19)$$

$$G_{cl}(s) = \frac{G_a(s)\times G_m(s)\times G_s(s)}{1+G_a(s)\times G_m(s)\times G_s(s)} = \frac{2}{2.5\,s^5 + 6.42\,s^4 + 2.962\,s^3 + 0.2363\,s^2+2} \quad (20)$$

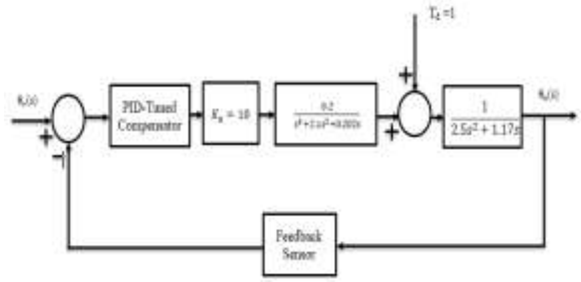

Figure 4: Closed loop network of satellite yaw-axis ACS with unit torque disturbance

$$G_L(s) = \frac{[G_a(s)\times G_m(s)+T_d(s)]G_s(s)}{1+[G_a(s)\times G_m(s)+T_d(s)]G_s(s)} = \frac{s^3+2.1s^2+0.202s+2}{2.5s^5+6.42s^4+3.962s^3+2.336s^2+0.202s+2} \quad (21)$$

2.2 Design of PID-Tuned Compensator

Symmetrical analysis, design, and tuning of linear control systems is provided by the control system designer (CSD) of the MATLAB/Simulink for industrial algorithms and applications (Muoghalu *et al*., 2020). Designing a compensator using CSD, can be achieved via PID tuning. Therefore, this section presents the design of PID-tuned compensator (PID-TC) for yaw-satellite ACS in CSD environment. The flowchart for the designing the PID-TC is shown in Figure 5.

© JUL 2026 | IRE Journals | Volume 10 Issue 1 | ISSN: 2456-8880
DOI: https://doi.org/10.64388/IREV10I1-1720170

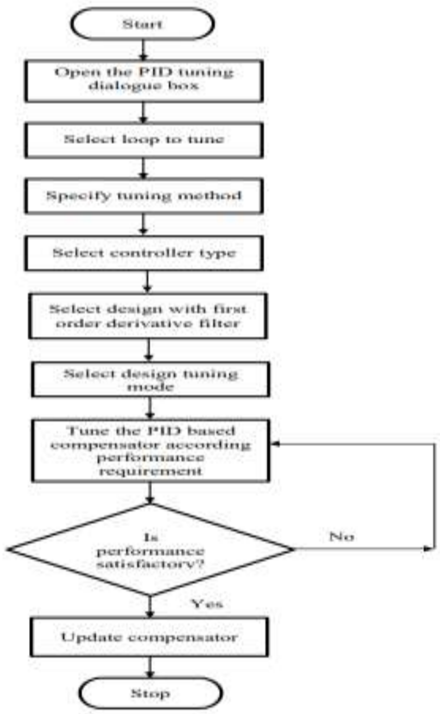

Figure 5: Design flowchart for the PID-TC

In designing the compensator, the tuning method chosen is the robust response time. The mode of design used is the frequency

Table 1: Parameters of the of yaw-axis ACS (Dorny, 2003; Ogata, 2003; Mbaocha et al., 2016)

Definition	Symbol	Value
Amplifier	K_a	10
motor a constant	K	0.01 Nm/A
Resistance of motor	R_a	1 Ω
Inductance of motor	L_a	0.5 H
Damping ratio of motor	B_a	0.01 Kgm^2
Moment of inertia of motor	J_a	0.1 Nms
Moment of inertia of satellite	J	2.5 Kg m^2
Damping ratio of satellite	B	1.17 Nms

III. RESULTS AND DISCUSSION

3.1 Uncontrolled System Analysis

This section presents the simulation analysis of the LEO satellite yaw-axis attitude dynamic when it is uncontrolled. In this scenario, it is assumed that no controller was introduced as a subsystem in the attitude control system (ACS). The essence of controller is to make sure that the satellite yaw angle (or attitude) is stabilized and tracked (or maintained) within the reference value while ensuring that the system performance criteria which include rapid convergence to stable and steady-state with little or no cycling, and zero or minimum deviation is attained. Thus in the absence of any controller, the step response of the LEO satellite yaw-axis ACS (uncontrolled system) is shown in Figure 6. This analysis was performed using the system model without the developed PID-TC controller. The resulting step response performance parameters of the uncontrolled system are listed in Table 2.

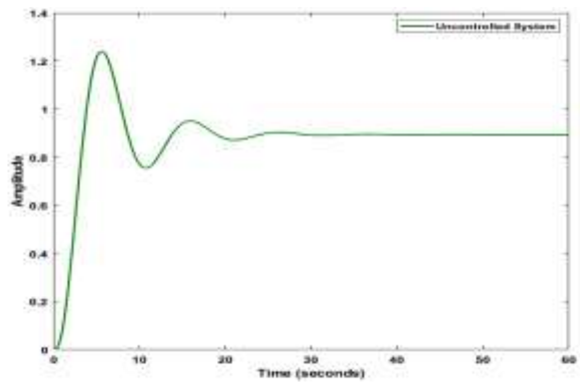

Figure 6: Step response of system without controller

Table 2: Step response performance characteristics of uncontrolled system

Step response parameter	Value
Rise time	2.16 s
Settling time	22.14 s
Peak time	5.62 s
Peak value	1.24
Overshoot	38.63%
Final value	0.89
Steady state error	0.11

From the step response shown in Figure 6, the dynamic response of the uncontrolled system to unit forcing input command revealed that it is characterized by rise time of 2.16 s, settling time of 22.14 s, peak time of 5.62 s, peak value of 1.24, overshoot of 38.63%, final value of 0.89 degree, and steady state error of 0.11. These performance parameters show that in uncontrolled state, the yaw-attitude of the satellite will take a long time (measured in terms of settling time) to settle or reach a stable state during on orbit flight operation. Even when it reach a steady-state, it does so at undesired or expected attitude (i.e. 0.89), which is less than the reference (or desired attitude taken as unit magnitude. This resulted in a steady-state error of 0.11, which is very much larger than the minimum value required of a control system usually 2% criterion in order to achieve stable and reliable operation. Generally, as shown in Figure 6, the curve revealed that the uncontrolled system was not able to achieve the desired attitude and suffers high instability as it overshoots the desired attitude by 38.63% (which is very much larger than the required 10%) at peak time of 5.62 s and reaching a peak value of 1.24 before settling at an attitude (0.89) very much less than the desired value (i.e. $0.89 \ll 1$). Therefore, there is need to develop a controller for on-orbit flight performance improvement in terms of reduced settling time, yaw-angle stability measured in terms of with very much reduced overshoot or zero, and reliable link operation measured in terms of little or no steady-state error.

3.2 Simulation Analysis of PID Tuned Compensator

This section presents the simulation scenario regarding the step response of the system when the PID tuned compensator (PID-TC) was introduced as a subsystem into the yaw-axis ACS. The simulation plot is shown in Figure 7 and the numerical analysis is shown in Table 3.

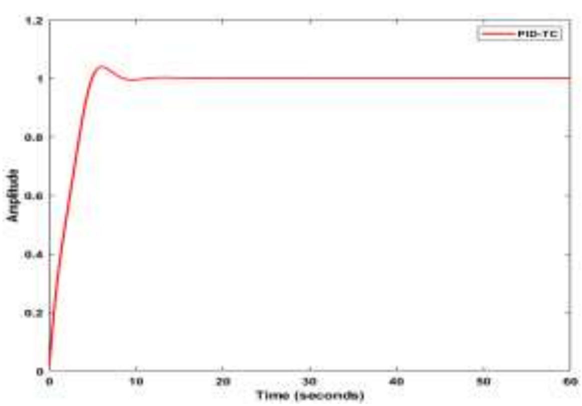

Figure 7: Step response of PID-TC yaw-axis ACS

Table 3: Step response performance characteristics of PID-TC system

Step response parameter	Value
Rise time	3.82 s
Settling time	7.30 s
Peak time	6.1 s
Peak value	1.04
Overshoot	3.88%
Final value	1.00
Steady state error	0.00

Looking at Figure 7, it can be observed that step response of the PID-TC control system overshoots or peaks the referenced unit attitude by 3.88% reaching a peak value of 1.04 at 6.1 s before settling at the referenced attitude at 7.30 s as shown in Table 3. The obtained dynamic response performance offered by the developed PID-TC is obviously within the acceptable required overshoot and settling time in terms of the performance specifications. It also represents an improvement over the uncontrolled system in settling time and overshoot. Also, the developed system offered zero steady-state error. This is an indication of its ability to provide reliable on-flight orbit operation with respect to the yaw-axis attitude determination.

3.3 Robustness Test of PID-TC with Unit Load Torque Disturbance

The robustness of the developed PID-TC was examined in this section by considering the presence of load torque disturbance on the dynamic response characteristics of the yaw-axis ACS. The step responses of the PID-TC based ACS and that with unit input load torque disturbance are shown in Figure 8. The resulting step response of the PID-TC with disturbance introduced in the control loop is tagged PID-TC-D. The parameters of the step response are listed in Table 4.

© JUL 2026 | IRE Journals | Volume 10 Issue 1 | ISSN: 2456-8880
DOI: https://doi.org/10.64388/IREV10I1-1720170

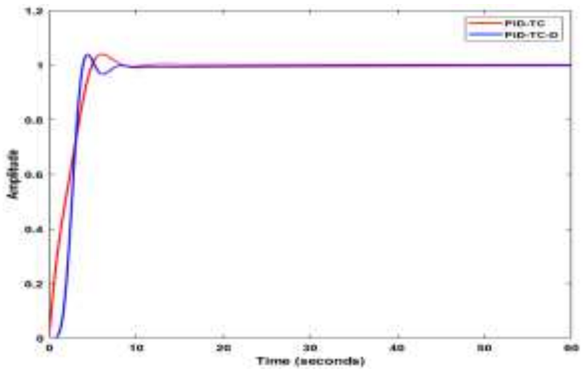

Figure 8: Step response of PID-TC ACS with and with disturbance

Table 4: Step response performance characteristics of PID-TC/PID-TC-D system

Step response parameter	PID-TC	PID-TC-D
Rise time	3.82 s	1.82 s
Settling time	7.30 s	6.90 s
Peak time	6.1 s	4.42 s
Peak value	1.04	1.05
Overshoot	3.88%	4.14%
Final value	1.00	0.997
Steady state error	0.00	0.003

Looking at Table 4, it can be seen that with the introduction of unit step load torque disturbance, PID-TC-D exhibited reduced rise (or response) time and settling time compared with PID-TC. This can be attributed to the fact that the presence of disturbance caused the controller (PID-TC) to rapidly response to applied input command in order to cancel the effect and converges or settles faster in order to restore the satellite at the appropriate yaw-axis attitude. However, the presence of the disturbance caused the system to further overshoot above the referenced attitude by 4.14% and reaching a slight increased peak value of 1.05 at time 4.42 s before it eventually settles at final attitude of 0.997. The resulting steady-state error is 0.003 (or 0.3%), which is very much less than the usually 2% (0.02) or 5% (0.05) criterion required of a control system. Thus, the steady-state error is approximately equal to zero. From this performance looking at Table 4, it is obvious that the developed system met the design specifications (i.e. overshoot of ≤ 5%, settling time of ≤ 10 s, and zero steady-error) in both control conditions. It can conclusively be said that the developed controller exhibits robustness in handling of perturbation in system dynamic behaviour.

3.4 Performance Comparison of Controllers

In this section, the developed yaw-axis ACS based on PID-TC is compared with other control techniques based implemented previously for LEO satellite as in Enerjor *et al*. (2023) and Mbocha *et al.* (2016), where PID and LQR have been applied. Simulation analysis was carried out initially when the ACS was without load torque disturbance as shown in Figure 9 and then with load disturbance as shown in Figure 10. The numerical values of the performance of the various systems are listed in Table 5 and 6 with respect to Figures 9 and 10.

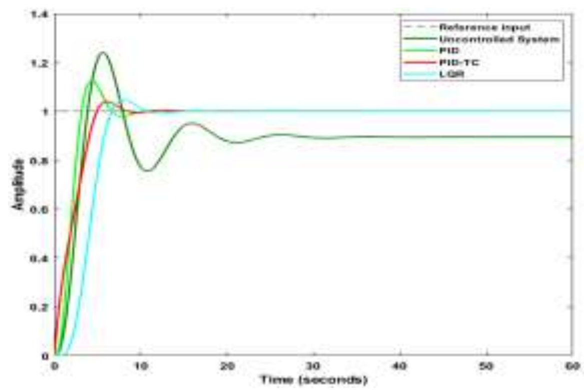

Figure 9: Comparison of ACS with different controllers (no disturbance)

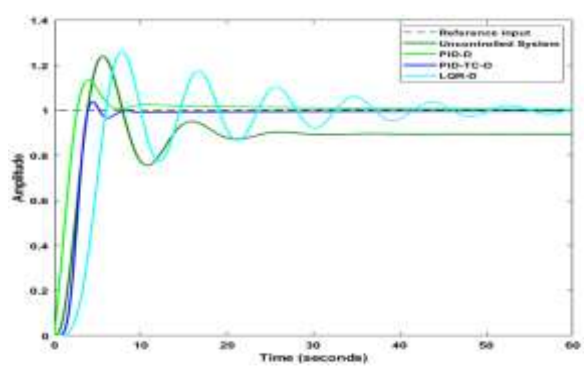

Figure 10: Comparison of ACS with different controllers (disturbance)

Table 5: Comparison of performance characteristics (no disturbance)

Step response parameter	Uncontrolled	PID	PID-TC	LQR
Rise time	2.16 s	1.95 s	3.82 s	3.53 s
Settling time	22.14 s	8.31 s	7.30 s	9.67 s
Peak time	5.62 s	4.35 s	6.1 s	8.02
Peak value	1.24	1.13	1.04	1.05
Overshoot	38.63%	12.51%	3.88%	4.74
Final value	0.89	1.00	1.00	1.00
Steady state error	0.11	0.00	0.00	0.00

Table 6: Comparison of performance characteristics (with disturbance)

Step response parameter	Uncontrolled	PID-D	PID-TC-D	LQR-D
Rise time	2.16 s	2.02 s	1.82 s	2.97 s
Settling time	22.14 s	11.9 s	6.90 s	57.32 s
Peak time	5.62 s	3.95 s	4.42 s	7.83 s
Peak value	1.24	1.13	1.05	1.26
Overshoot	38.63%	12.84%	4.14%	25.72%
Final value	0.89	1.00	0.997	1.00
Steady state error	0.11	0.00	0.003	0.00

From Figure 9 and Table 5, it can be seen that the introduction of the only the developed PID-TC and the LQR controllers met the specifications for the dynamic response of the yaw-axis ACS. Though, the PID met the specified settling time, its overshoot was 12.51% above the desired or referenced attitude. Also, the PID-TC provided the best performance in terms of in terms of settling time and overshoot. This means that the developed system offered faster convergence, smoother and stable torque control performance than the other controllers. Further comparison in terms of the ability to offer robustness in the presence disturbance with respect Figure 10 and Table 6, revealed that the PID-TC outperformed the PID and LQR. The LQR showed the worst performance in the presence of disturbance. Therefore, it suffices to say that the developed PID-TC outperformed the existing PID and LQR controllers.

IV. CONCLUSION

This paper has presented enhancing the stabilization of low earth orbit satellite yaw-axis attitude control system using robust proportional-integral-derivative-tuned compensator (PID-TC). In order to realize the aim of this work, the dynamic equations representing the behaviour of a microsatellite yaw-axis in attitude control system were determined. The dynamic equations were then modelled using Simulink embedded blocks in MATLAB. A PID-TC was developed to provide command action for LEO satellite yaw-axis ACS. The developed control system was modelled and simulated in MATLAB/Simulink environment. The results from the simulation revealed that the developed system met the performance specifications of the LEO satellite yaw-axis ACS particularly yielding very much reduced oscillation in terms of overshoot and zero steady-state error. This indicates improved stabilization of the satellite compared to its overshoot (38.63%) when the PID-TC has not been introduced. The system performance was measured in terms of time domain transient characteristics such as rise time, transient time, settling time, maximum overshoot, peak time, final value and steady state error. The effectiveness of the developed system was further examined for robustness in the presence of disturbance. The outcome revealed that the design specifications were achieved even in the presence disturbance. Furthermore, comparing it with other strategies, it was observed that the PID-TC system yielded the best performance having met the performance criteria and provides the most reduced overshoot that signifies near absence of oscillation in satellite operation in its yaw-axis and improved stability. Generally, considering the time domain characteristic of the various system responses from the different controller to unit load torque disturbance, it suffices to say that the introduction of the designed PID-TC controller largely enhanced the ACS performance.

ACKNOWLEGDEMENT

The authors expressed sincere gratitude to the staff of the Department of Electrical/Electronic Engineering, Chukwuemeka Odumegwu Ojukwu University, Uli Campus for access to its laboratories used in this study.

REFERENCES

[1] Achebe, P. N. & Muoghalu, C. N. (2025). Design of adaptive PD controller for microsatellite yaw axis attitude control system. *International Journal of Engineering Research and Development, 21*(2), 225-232.

[2] Ajiboye, A. T., Popoola, J. O., Oniyide, O., &Ayinla, S. L. (2020). PID controller for microsatellite yaw-axis attitude control system using ITAE method. *TELKOMNIKA Telecommunication, Computing, Electronics and Control, 18*(2), 1001-1011. DOI: 10.12928/TELKOMNIKA.v18i2.14303

[3] Akwukwaegbu, I. O., Nosiri, O., Olubiwe, M., Paulinus Nwammuo, C. F., Okonkwo, E. (2023). Design of model following control integrating PID controller for DC servomotor-based antenna positioning system. *SSRG International Journal of Electrical and Electronic Engineering, 10*(6), 33-42.

[4] Benzeniar, H. & Fellah, M. K. (2014). A microsatellite reaction wheel based on a fuzzy logic controller for the attitude control system. *International Review in Aerospace Engineering,* 7(5), 54-63. https://doi.org/10.15866/1rease.v7i5.4973

[5] Dorny, C. N. (2003). Understanding dynamic systems: approaches to modeling, analysis and design, Prentice-Hall,

[6] Enejor, E.U., Dahunsi, F. M., Akingbade, K. F., & Nelson, I. O. (2023). Low Earth orbit satellite attitude stabilization using linear quadratic regulator. *European Journal of Electrical Engineering and Computer Science, 7*(3), 17-29.

[7] http://dx.doi.org/10.24018/ejece.2023.7.3.505

[8] Eze, P. C., & Ezenugu, I. A. (2024). Microsatellite yaw-axis attitude control system using model reference adaptive control based PID controller. *International Journal of Electrical Computer Engineering Research*, 4, 8-16.

[9] Eze P. C., Ugoh C. A., Inaibo D. S. (2021). Positioning control of DC servomotor-based antenna using PID tuned compensator. *Journal of Engineering Sciences, 8*(1), pp. E9–E16, doi: 10.21272/jes.2021.8(1).e2

[10] Eze, P. C., Onuora, A. E., Ekengwu, B. O., Muoghalu, C., & Aigbodioh, F. A. (2017). Design of a robust PID controller for improved transient response performance of a linearized engine idle speed model. *American Journal of Engineering Research*, 6(8), 305-313.

[11] Jin, L., & Li, Y. (2022). Model predictive control-based attitude control of under-actuated spacecraft using solar radiation pressure. *Aerospace, 9*, 498, 1-20.

[12] https://doi.org/10.3390/aerospace9090498

[13] Mbaocha, C. C., Eze, C. U., Ezenugu, I. A., & Onwumere, J. C. (2016). Satellite model for yaw-axis determination and control using PID compensator. *International Journal of Scientific & Engineering Research, 7*(7), 1623-1629.

[14] Muoghalu, C. N. & Achebe, P. N. (2021). Two-phase hybrid stepping motor based antenna positioning control system using proportional integral and derivative controller. *Iconic Research and Engineering*, 4(10), 152-157.

[15] Muoghalu C.N. & Achebe P.N. (2025). Enhancing the dynamic response servo positioning system using internal model control based compensator: A case study of HDD. *International Journal of Progressive Research in Engineering Management and Science,* 5(3), 236-242.

[16] Muoghalu, C.N., Achebe, P.N., & Okafor, C.S. (2024). Human heart stabilization using mathematical based model with proportional integral and derivative controller. *International Journal of Latest Technology in Engineering, Management and Applied Science*, XIII(III), 1-9.

[17] Muoghalu, C. N., Ndefo, M. I., & Ugwu, H. I. (2021). Performance enhancement of chopper fed DC motor speed control system using PID controller. *Multidisciplinary International Journal of Research and Development*, 1(2), 1-8.

[18] Muoghalu, C. N., Uju, I. U., & Mbachu, C. B. (2020). Performance improvement of automatic voltage regulator using linear quadratic Gaussian tuned controller. *International Journal of Latest*

Technology in Engineering, Management & Applied Science, 9, 96-12.

[19] Ogata, K. (2003). System dynamics, 4th ed. Prentice-Hall, Englewood Cliffs, New Jersey, 2003.

[20] Okasha, M. Idres, M., &Ghaffar, A. (2019). Satellite attitude tracking control using Lyapunov control theory. *International Journal of Recent Technology and Engineering, 7*(6S), 253-257.

[21] Okeya, D. C. C., Mbachu, C. B., Muoghalu, C. N., & Ekengwu, B. O. (2024). Enhancing the pitch control of an unmanned aircraft using PSO based intelligent PID controller. *International Journal of Research Publication and Reviews,* 5(3), 55-63.

[22] Onyeka E. B., Chidiebere M., & Nkiruka A. P. (2019). Improved response performance of two-phase hybrid stepping motor control using PID tuned outer and inner loop compensator. *Journal of Engineering Sciences,* 6(1), D1-D6.

[23] Onyekwelu, C. I., Nwabueze, C. A., Muoghalu, C. N., & Ekengwu, B. O. (2023). Model reference adaptive control based PID controller for hard disk drive read/write head servo positioning system. *International Journal of Academic Multidisciplinary Research*, 7(8), 135-144.

[24] Qi, Y., Jing, H., & Wu, X. (2022). Variable structure PID controller for satellite attitude control considering actuator failure. *Applied Sciences, 12*, 5273, 1-19. https://doi.org/10.3390/app12105273

[25] Shan, Y., Xia, L., & Li, S. (2022). Design and simulation of satellite attitude control algorithm based on PID. *Journal of Physics: Conference Series, 2355* 012035. DOI:10.1088/1742-6596/2355/1/012035